

A Minimally Invasive Method for Beat-by-Beat Estimation of Cardiac Pressure-Volume Loops

Shaun Davidson¹, Chris Pretty¹, Shun Kamoi¹, Thomas Desaive² and J. Geoffrey Chase¹

¹*Department of Mechanical Engineering, University of Canterbury, Christchurch, New Zealand*

²*GIGA-Cardiovascular Sciences, University of Liège, Liège, Belgium*

Keywords: Pressure-Volume Loops, Cardiovascular Signals, Clinical Monitoring, Stroke Work.

Abstract: This paper develops a minimally invasive means of estimating a patient-specific cardiac pressure-volume loop beat-to-beat. This method involves estimating the left ventricular pressure and volume waveforms using clinically available information including heart rate and aortic pressure, supported by a baseline echocardiography reading. Validation of the method was performed across an experimental data set spanning 5 Piétrain pigs, 46,318 heartbeats and a diverse clinical protocol. The method was able to accurately locate a pressure-volume loop, identifying the end-diastolic volume, end-systolic volume, mean-diastolic pressure and mean-systolic pressure of the ventricle with reasonable accuracy. While there were larger percentage errors associated with stroke work derived from the estimated pressure-volume loops, there was a strong correlation (average R value of 0.83) between the estimated and measured stroke work values. These results provide support for the potential of the method to track patient condition, in real-time, in a clinical environment. This method has the potential to yield additional information from readily available waveforms to aid in clinical decision making.

1 INTRODUCTION

Cardiovascular disease and dysfunction (CVD) was responsible for 31% of global deaths in 2013 (Mozaffarian et al., 2015), and continues to be a leading worldwide cause of Intensive Care Unit (ICU) admission and mortality. The global cost of CVD was an estimated \$863 billion USD in 2010, equivalent to 1.39% of gross world product (Mozaffarian et al., 2015). Incorrect or inadequate diagnosis of cardiac dysfunction contributes to these statistics, potentially increasing ICU length of stay, cost and mortality (Angus et al., 2001, Pineda et al., 2001). With these figures expected to rise with aging populations, there is a clear need for optimised, patient-specific cardiovascular care to mitigate the social and economic burden.

Management of cardiac patients in the ICU often utilises information from catheters placed in the arteries and veins around the heart. Despite their information rich nature, the use of such catheters is not necessarily associated with improved clinical outcomes (Frazier and Skinner, 2008, Chatterjee, 2009). There is thus potential for new methods to more effectively extract cardiac information from

these catheter signals, yielding further value from readily available data that has potentially been under-utilised to date.

The Pressure-Volume (PV) loop is one of the fundamental means of expressing internal cardiac dynamics and function (Hall, 2010). A PV loop is formed by plotting ventricular pressure and volume for a heartbeat. The area within the PV loop is equivalent to stroke work, the work done by the heart to eject blood into the aorta (Suga, 1990, Burkhoff and Sagawa, 1986). Stroke work is an important metric that changes in response to cardiac dysfunction. Further, the location of the PV loop provides information about contractility (Suga et al., 1973, Broscheit et al., 2006), which is similarly sensitive to changes in cardiac state and function.

Unfortunately, PV loops cannot be directly measured in clinical practice, as this would require placing catheters directly into the heart chambers. Hence, the use of PV loops is mainly limited to experimental and conceptual work. Clinically, there has been interest in curves and metrics derived from the PV loop, such as the End-Systolic Pressure-Volume Relation (ESPVR) (Suga et al., 1973), the Stroke Work to End-Diastolic Volume Relation

(Little et al., 1989) and the dP/dt_{\max} to End-Diastolic Volume Relation (Little, 1985).

Accordingly, there has been various work towards clinically estimating these relationships and their associated properties. However, these methods typically focus on individual components such as ESPVR (Senzaki et al., 1996, Chen et al., 2001), End-Diastolic Pressure Volume Relation (EDPVR) (Klotz et al., 2006) or Preload Recrutable Stroke Work (PRSW) (Karunanithi and Feneley, 2000, Lee et al., 2003), as such they fail to provide the comprehensive and unified set of information about cardiac dynamics provided by a PV loop. Further, these methods typically rely on continuous echocardiography, which is not practical for ICU wide implementation due to the current cost of these systems (Ferrandis et al., 2013). There has been little work associated with non-invasive estimation the PV loop itself to date.

This paper presents a novel method of non-invasively estimating the beat-by-beat PV loop. The method combines simple physiological assumptions with clinically available catheter waveforms to individually estimate the pressure and volume components of the PV loop. Clinically feasible measurements mean the method has the potential for real-time implementation at the bedside, without additional invasive instrumentation. These PV loops could be used to provide additional, patient specific information on intra-beat behaviour and inter-beat variation in the functioning of the heart.

2 METHODS AND ANALYSIS

2.1 Proposed Method

The left ventricular PV loop is generated from two waveforms, the left ventricular pressure (P_{lv}) and left ventricular volume (V_{lv}). Both waveforms can be directly measured, but doing so is not clinically feasible (Kastrup et al., 2007). The proposed method approximates these two waveforms (P_{lv} , V_{lv}) using three inputs, as shown in Fig. 1 Two of these inputs, a continuously sampled aortic pressure waveform (P_{ao}) and heart rate (HR), are typically available in a modern ICU. The third input, baseline End-Systolic (V_{es}) and End-Diastolic (V_{ed}) Volume, may be clinically obtained from a brief echocardiography reading, which is increasingly clinically available (Viellard-Baron et al., 2008). The continuous pressure measurement (P_{ao}), situated directly downstream from the ventricle, is an effective basis to estimate P_{lv} . However, there is no similar measurable volume waveform from which to estimate

V_{lv} , resulting in the relative complexity of the shaded region in Fig. 1.

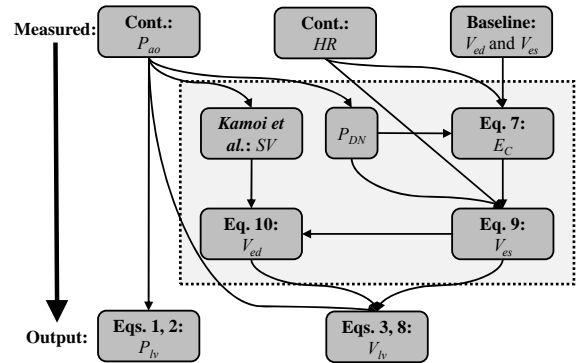


Figure 1: Summary flowchart of the proposed method.

This method encompasses the estimation of two output waveforms (V_{lv} , P_{lv}) using one input waveform (P_{ao}). It is important to note that this goal can only be effectively accomplished because all three waveforms (P_{lv} , V_{lv} , P_{ao}) consist of different regions of behaviour governed by different physiological phenomena, and have been extensively characterised (Hall, 2010). More specifically, these three waveforms are both rich in information and heavily interconnected.

2.1.1 Estimating P_{lv} from P_{ao}

The aortic valve separates the left ventricle (upstream) from the aorta (downstream). The valve opens during systole, as blood is ejected from the ventricle into the aorta, and closes during diastole, while the ventricle fills. Provided aortic valve resistance is negligible, P_{lv} can be assumed to be equivalent to P_{ao} while the aortic valve is open (Section P.1, Fig 2), subject to a slight phase lag (δ).

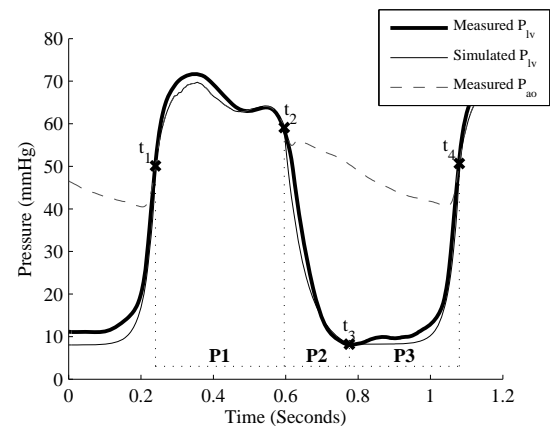


Figure 2: Estimating left ventricular pressure, note P_{ao} has been shifted left by δ .

When the aortic valve is closed during diastole, P_{ao} and P_{lv} diverge significantly. However, as the ventricle relaxes and fills during diastole, its behaviour in this region is largely passive (Hall, 2010). Diastolic P_{lv} was thus approximated using a pair of generic exponential functions. The first simulates ventricular relaxation during early diastole (Section P. 2, Fig. 2) to a fixed baseline pressure. The second captures the beginning of ventricular contraction in late diastole-early systole (Section P. 3, Fig. 2). Atrial behaviour is neglected in this model.

Per Fig. 2, P_{lv} for the n_{th} heartbeat is thus defined:

$$t_1 = t \left(\frac{dP_{ao}}{dt}_{max} \right)_n \quad (1a)$$

$$t_2 = t \left(\frac{dP_{ao}}{dt}_{min} \right)_n \quad (1b)$$

$$t_4 = t \left(\frac{dP_{ao}}{dt}_{max} \right)_{n+1} \quad (1c)$$

$$t_3 = 0.62t_2 + 0.38t_4 \quad (1d)$$

$$P_{lv}(t) = \begin{cases} P_{ao}(t_1 + \delta < t < t_2 + \delta) & t_1 \\ 6 + (P_{ao}(t_2) - 6)e^{-17.5(t-t_2)} & t_2 \\ P_{lv}(t_3) + (P_{ao}(t_4) - P_{lv}(t_3))e^{37.5(t-t_4)} & t_3 \end{cases} \quad (2)$$

where: $\delta = 0.008s$

2.1.2 Estimating V_{lv} from P_{ao} and HR

Estimating V_{lv} is significantly more complicated than P_{lv} due to the lack of volume or flow information readily available from typical clinical instrumentation. V_{lv} was estimated by selecting a generic waveform and then locating the timing and magnitude of the peaks and troughs of this waveform on a beat-by-beat basis. The generic waveform consisted of a piecewise sine wave broken down into two sections: systole (Section V. 1, Fig. 3) and diastole (Section V. 2, Fig. 3), with a 90° phase shift at the beginning of systole. While the underlying behaviour of the ventricle might be better represented by a series of exponentials (Hall, 2010), the use of sine waves achieves a similar results in Fig. 3, while requiring considerably fewer variables.

To locate the waveform peaks and troughs, six points per heartbeat are required (t_1 , t_2 , t_3 and $(V_{ed})_n$, $(V_{es})_n$, $(V_{ed})_{n+1}$). The timing associated with systole start (t_1), systole end (t_2), and diastole end (t_3) are readily determined from the aortic pressure waveform (Fig. 3):

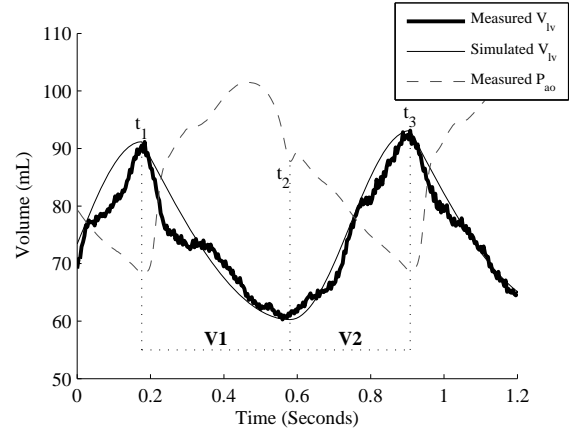


Figure 3: Estimating left ventricular volume.

$$t_1 = t(P_{ao_{min}})_n \quad (3a)$$

$$t_2 = t(P_{DN})_n \quad (3b)$$

$$t_3 = t(P_{ao_{min}})_{n+1} \quad (3c)$$

Finding the magnitude of these peaks and troughs is more involved. For a given heartbeat, stroke volume (SV) can be approximated from the aortic waveform per (Kamoi et al., 2014), relating V_{es} and V_{ed} . The End-Systolic PV Relation (ESPVR) can be used to find V_{es} (Sagawa, 1981):

$$P_{es} = E_{es} \times (V_{es} - V_0) \quad (4)$$

where E_{es} is the end-systolic elastance and V_0 is the ventricular volume at zero pressure. Eq. 4 can be rewritten:

$$P_{DN} = E_{es} \times (V_{es} - V_d) \quad (5)$$

where this change is justified by:

- The pressures in the ventricle and aorta, as previously mentioned, can be assumed to be similar while the aortic valve is open, thus P_{DN} can be used a surrogate for P_{es}
- V_d and V_0 have similar physiological definitions and values, and the two are frequently used interchangeably (Sagawa, 1981, Stevenson et al., 2012b, Stevenson et al., 2012a). It is possible to approximate baseline V_d as a fixed percentage of baseline V_{es} (Davidson et al., 2016), which is available during the initial echocardiographic reading. V_d is known to change with condition, but such changes cannot be captured without additional echocardiography readings. While such intermittent measures are feasible, V_d is fixed at its baseline value in this study.

$$V_d = 0.48 \times V_{es} \quad (6)$$

Finally, it is necessary to account for E_{es} , which changes in response to loading conditions (Burkhoff et al., 1993, Baan and Van Der Velde, 1988) and contractility (Suga et al., 1973). To approximate these changes, Eq. 5 is modified:

$$P_{DN} = (E_c \times HR^3) \times (V_{es} - V_d) \quad (7)$$

where E_{es} is approximated as a function of heart rate (HR) and a coefficient (E_c). A single term power relation was selected as it can be explicitly defined during the echocardiography calibration, and provides reasonable effective tracking for the data set presented here. Changes in both E_{es} and HR are staple cardiovascular system responses to most changes in conditions (Hall, 2010). As heart rate is continuously monitored in most modern ICUs, it provides an easily obtained, but only partial, indication of cardiovascular system response to inform an approximated elastance. Further supporting evidence is provided in the validation and discussion of results.

During the echocardiography calibration, measurements for P_{DN} , HR and V_{es} are available (Lang et al., 2015). Thus, a constant value for E_c can be defined (Eq. 7), enabling beat-by-beat approximation of E_{es} and thus V_{es} . The beat-to-beat ventricular volume can thus be estimated:

$$V_{lv}(t) = \begin{cases} (V_{ed})_n + ((V_{es})_n - (V_{ed})_n) \sin\left(\frac{\pi(t-t_1)}{2(t_2-t_1)}\right) & t_1 < t < t_2 \\ (V_{es})_n - ((V_{ed})_{n+1} - (V_{es})_n) \left(\frac{1}{2} \cos\left(\frac{\pi(t-t_2)}{(t_3-t_2)}\right) - \frac{1}{2}\right) & t_2 < t < t_3 \end{cases} \quad (8)$$

where:

$$V_{es} = \frac{P_{DN}}{(E_c \times HR^3)} + V_d \quad (9)$$

$$V_{ed} = V_{es} + SV \quad (10)$$

2.1.3 Summary of Proposed Method

The overall derivation of the driver function, also in Fig. 1, can be summarised:

Initially or Intermittently:

1. Calculate V_d using Eq. 6 and baseline V_{es}
2. Calculate E_c using Eq. 7, P_{DN} , HR and baseline V_{es}

Every heartbeat:

1. Simulate P_{lv} using Eq. 1, Eq. 2 and P_{ao}
2. Determine V_{es} using Eq. 9, P_{DN} , HR and E_c
3. Determine SV using (Kamoi et al., 2014) and P_{ao}
4. Determine V_{ed} using Eq. 10, V_{es} and
5. Simulate V_{lv} using Eq. 3, Eq. 8, P_{ao} , V_{es} and V_{ed}
6. Use P_{lv} and V_{lv} to generate the PV loop

2.2 Analysis and Validation

The performance of the proposed method was evaluated over an experimentally gathered data set, consisting of continuously measured method inputs (P_{ao}) and outputs (V_{lv} , P_{lv}). This data set allowed validation of the ability of the method to individually estimate P_{lv} and V_{lv} , as well as validation of the overall method through comparisons between estimated and directly measured PV loops. The data set includes a total of 46,318 heartbeats across 5 Piétrain pigs, measured across a clinical protocol designed to provide diverse cardiac conditions.

2.2.1 Experimental Procedure

Five male, pure Piétrain pigs weighing between 18.5 and 29 kg were subject to a protocol approved by the Ethics Commission for the Use of Animals at the University of Liège, Belgium. The pigs were sedated, anaesthetised and mechanically ventilated (GE Engstrom CareStation) with a baseline positive end-expiratory pressure (PEEP) of 5 cmH₂O. The heart was accessed via a median sternotomy, and an admittance PV catheter (Transonic, NY, USA) with a sampling rate of 250 Hz inserted into the left ventricle. Proximal aortic pressure was continually sampled using a pressure catheter (Transonic, NY, USA) with a sampling rate of 250 Hz.

To ensure a diverse range of cardiac states was exhibited, several procedures were performed:

- A single infusion of endotoxin (lipopolysaccharide from E. Coli, 0.5 mg/kg injected over 30 minutes) to induce septic shock, which drives a change in afterload conditions and is associated with a large variety of effects including an inflammatory response and capillary leakage that may lead to hypovolemia, global tissue hypoxia and cardiac failure (Nguyen et al., 2006).
- Several PEEP driven recruitment manoeuvres (RMs), both pre- and post- endotoxin infusion, which drive a change in preload conditions and are typically associated with a decrease in mean blood pressure and cardiac output (Jardin et al., 1981).
- 1 – 4 infusions of 500 mL saline solution over 30 minute periods, pre- and post- endotoxin infusion, simulating fluid resuscitation therapy, a key component of hemodynamic resuscitation in patients with severe sepsis, which itself results in a change in circulatory volume (Vincent and Gerlach, 2004).

2.2.2 Model Validation

The overall method presented here is designed to simulate the left ventricular PV loop beat-by-beat, without requiring additionally invasive instrumentation of the heart or continuous real-time image-based monitoring, neither of which is clinically or ethically feasible in care. As such, validation of the method relies on comparison of the simulated PV loop to the invasively measured, ‘true’ PV loop.

The important information contained in a PV loop can be broadly broken down into its shape and enclosed area, as well as the absolute (P , V) position of the loop. Comparison of the estimated and measured PV loops thus encompasses several metrics:

- **Mean Pressures:** A comparison between measured and estimated mean systolic and diastolic pressures for each heartbeat (P_{sys} , P_{dia}).
- **Volumes:** A comparison between the measured and estimated end-systolic volume (V_{es}) and end-diastolic volume (V_{ed}) for each heartbeat.
- **Stroke Work:** A comparison of the area enclosed within a given pressure volume loop.

Each comparison involves an evaluation of the beat-by-beat percentage errors between the measured and estimated values of the relevant metric. Estimated stroke work values were also compared to stroke work approximated by equation:

$$SW_E = SV \times MSP \quad (11)$$

where MSP is the mean systolic pressure in the aorta and SV the stroke volume of a given heartbeat. Eq. 11 is a lumped approximation of stroke work (Klabunde, 2011). Finally, the linear correlation between the measured and simulated stroke work was evaluated using Pearson’s correlation coefficients.

3 RESULTS

3.1 Pressure and Volume

Per Eq. 2, the systolic pressure is primarily a function of phase shifted P_{ao} , while the diastolic pressure is primarily a function of fixed waveforms. Thus, the errors presented in Table 1 provide a means to validate both the performance of the overall method, as well as the specific assumptions involved with estimating the different regions of P_{lv} . The extremely low errors for P_{sys} , with medians of 1.5-12.1% suggest that, as would be physiologically expected, P_{ao} provides an effective estimate for systolic

ventricular pressure. The errors associated with P_{dia} are somewhat higher, but it should be noted that these are percentage errors and values for P_{dia} are often an order of magnitude smaller than those of P_{sys} . As such, median errors ranging from 6.4-23.8% for generic exponential functions still imply the method is functioning reasonably effectively.

Table 1: Percentage errors associated with pressure estimation, median (25th percentile – 75th percentile).

Pig	Abs. Error: Mean-Diastolic Pressure (P_{dia})	Abs. Error: Mean-Systolic Pressure (P_{sys})
Pig 1	23.3% (8.5 – 30.7)	7.1% (4.8 – 10.4)
Pig 2	6.4% (2.9 – 12.9)	1.5% (0.6 – 2.6)
Pig 3	13.4% (5.8 – 19.8)	1.7% (1.1 – 2.6)
Pig 4	17.4% (12.8 – 26.2)	12.1% (10.1 – 13.7)
Pig 5	23.8% (14.9 – 31.2)	2.2% (1.3 – 4.2)
Average	16.9% (9.0 – 24.2)	4.9% (3.6 – 6.7)

Per Eq. 8, the end-systolic volume is a function of a variety of assumptions made in deriving a modified ESPVR (Eq. 7). Thus the errors presented in Table 2 serve as an excellent means of validating this body of assumptions. The end-diastolic volume, per Eq. 10, combines the assumptions made in deriving V_{es} with those made in deriving SV as in (Kamoi et al., 2014). The results in Table 2 thus provide a means of approximating the contribution to error of the various assumptions and equations involved in estimating V_{lv} . The errors associated with V_{es} are low, with median values ranging from 2.0-6.6%. This result implies that the assumptions concerning simulating E_{es} using HR and V_d using baseline V_{es} are, at least, effective over the data set evaluated. The errors for V_{ed} are slightly greater, with medians ranging from 4.5-13.2%. This error is still within a very acceptable level, especially when one considers it combines error contributions from estimation of both V_{es} and SV . Overall, the results in Tables 1 and 2 suggest the method is able to effectively locate a PV loop.

Table 2: Percentage errors associated with pressure estimation, median (25th percentile – 75th percentile).

Pig	Abs. Error: End-Systolic Volume (V_{es})	Abs. Error: End-Diastolic Volume (V_{ed})
Pig 1	2.0% (1.0 – 3.3)	4.5% (1.5 – 8.8)
Pig 2	6.6% (4.4 – 9.9)	13.2% (4.9 – 17.5)
Pig 3	4.5% (2.6 – 7.6)	6.2% (2.9 – 12.0)
Pig 4	4.7% (2.2 – 8.1)	5.6% (3.1 – 11.0)
Pig 5	4.3% (2.5 – 8.1)	5.3% (3.0 – 9.9)
Average	4.4% (2.5 – 7.4)	7.0% (3.1 – 11.8)

3.2 Stroke Work

Table 3 presents the percentage errors in stroke work

for different approximations compared to stroke work derived from the directly measured V_{lv} and P_{lv} waveforms. Estimated stroke work represents stroke work derived from the estimated PV loop, while simplified stroke work uses Eq. 11. As highlighted by the bolded values, the estimated method produced lower percentage errors in 11 of the 15 metrics assessed, and lower overall average error values. However, the estimated method did produce mildly higher 25th percentile and median errors for Pig 2, and significantly higher (though still relatively low) 25th percentile and median errors for Pig 4.

Table 3: Percentage errors associated with stroke work estimation, median (25th percentile – 75th percentile).

Pig	Abs. Error: Estimated Stroke Work (SW_E)	Abs. Error: Simplified Stroke Work (SW_S)
Pig 1	15.6% (5.3 – 21.3)	30.6% (7.5 – 39.1)
Pig 2	16.4% (10.4 – 20.7)	14.3% (7.6 – 24.0)
Pig 3	24.6% (12.4 – 42.9)	43.1% (22.5 – 67.6)
Pig 4	41.2% (14.2 – 61.1)	57.4% (25.0 – 74.8)
Pig 5	20.8% (17.5 – 55.6)	8.9% (4.7 – 96.4)
Average	23.6% (12.0 – 40.3)	30.9% (13.5 – 60.4)

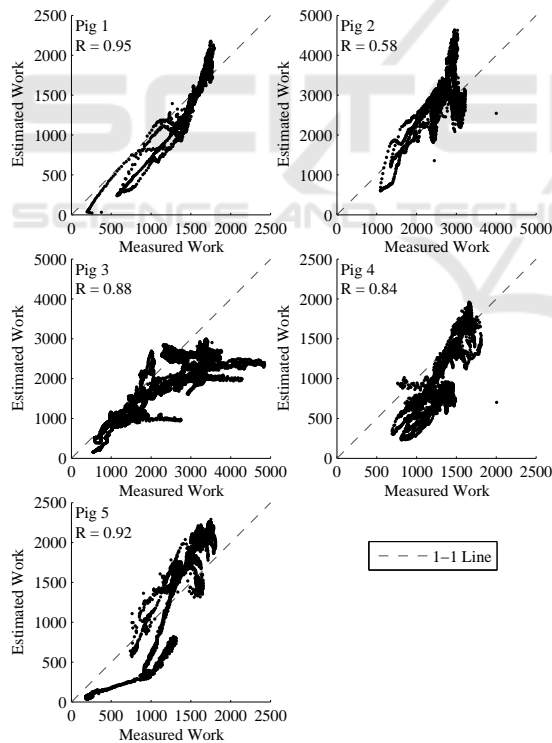


Figure 4: Correlation plots for estimated and measured stroke work.

Fig. 4 presents correlation plots between the

estimated and directly measured stroke work. The correlation coefficients are generally high, with an average of $R = 0.83$. The exception to this is Pig 2, with a correlation coefficient of just $R = 0.58$. Regardless, these results show a generally strong link in trends between simulated and measured stroke work values, combined with the improvement in percentage error values over a current approximation method in Table 3, provide support for the applicability of this method.

Fig. 5 presents a set of example measured and estimated PV loops for each of the 5 pigs. The three PV loops presented for each pig are designed to provide examples representative of 25th percentile, median and 75th percentile error for that pig. As can be seen from these example PV loops, the method does a reasonable job of capturing the range of distinct shapes the PV loop assumes as condition and subject changes. Additionally, in support of the results in Tables 1 and 2, the method locates the PV loops with relative accuracy, even when stroke work errors are relatively high.

4 DISCUSSION

4.1 Pressure and Volume

The pressure and volume results summarised in Tables 1 and 2 provide both a means of validating the ability of the method to correctly locate the PV loop, as well as a means of validating various model assumptions and evaluating their contribution to error. The low errors for P_{sys} in Table 1 suggest the phase shifted P_{ao} effectively simulates systolic ventricular pressure, and this ‘edge’ of the PV loop is effectively captured. The higher errors for P_{dia} in Table 1 are expected due to the generic nature of the exponentials used to simulate systolic ventricular pressure. However, given the relatively low magnitude of these values, the 6.4-23.8% median errors observed do not correspond to a significant absolute deviation in this ‘edge’ of the PV loop.

Estimation of V_{lv} was significantly more challenging. However, the errors in Table 3 are very comparable to those presented in Tables 1 – 2. Errors associated with V_{es} are relatively low, with medians of 2.0-6.6%. These low values are important, because V_{es} is a product of both the assumption that V_d can be approximated from baseline V_{es} (Eq. 6) and that elastance can be approximated as a function of HR (Eq. 7), both of which are significant assumptions.

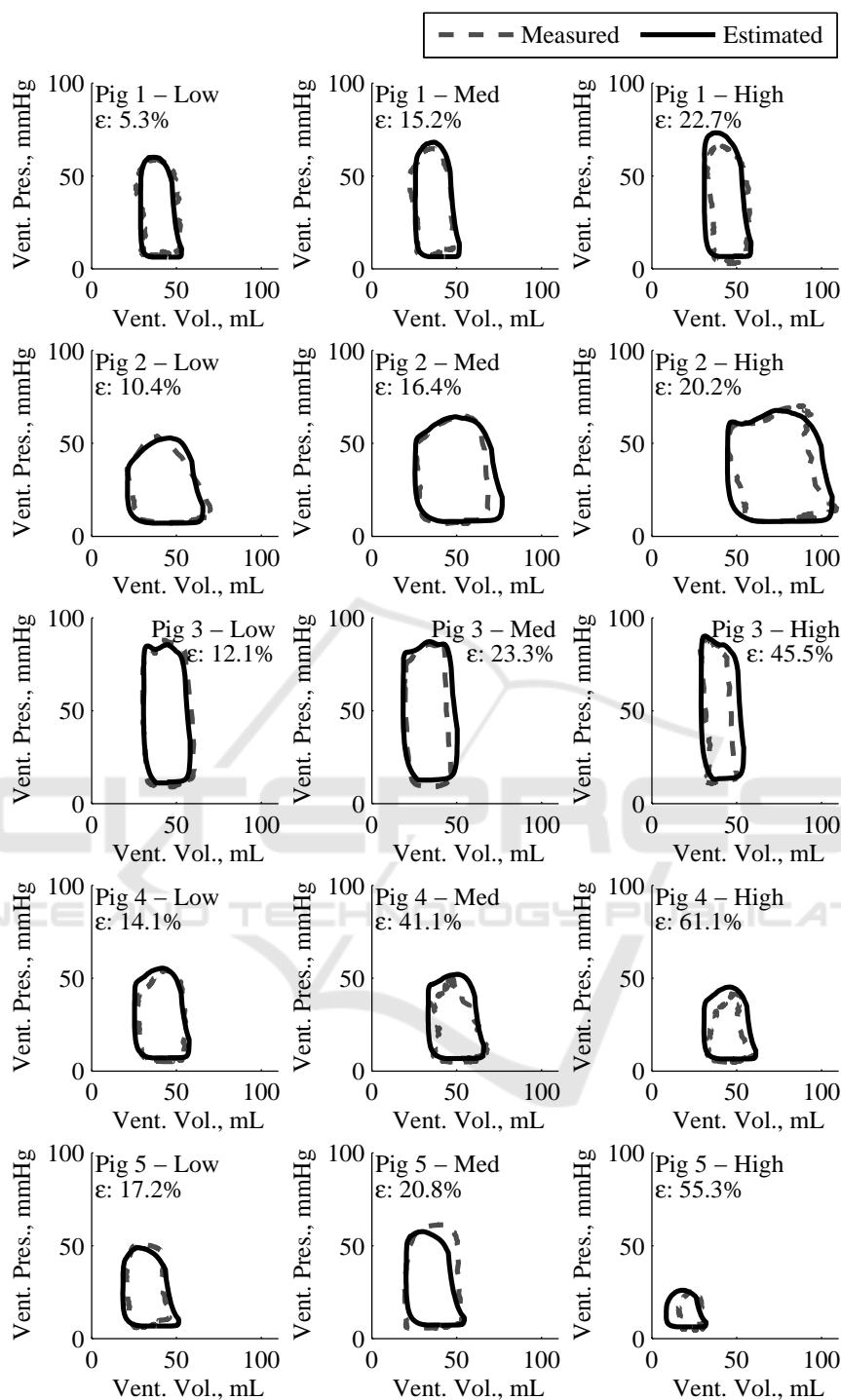


Figure 5: Example measured and estimated PV loops for different error quartiles from all 5 pigs.

Errors associated with V_{ed} are slightly larger, with medians 4.5-13.2%. These results are very acceptable considering they combine the error contributions from the method of deriving V_{es} with the error contributions from estimating SV per (Kamoi et al.,

2014). Regardless, all of the specified errors appear well within acceptable margins, suggesting the method should be able to accurately locate the PV loop.

It is still important to note the assumptions made, specifically in Eq. 7, represent a significant simplification of actual cardiac behaviour. The power function used to estimate E_{es} from HR attempts to capture the sympathetic component of cardiac system response. Inevitably, though this sympathetic relationship varies between individuals, accounted for here by calibration, and with changes in condition and time. While this approximation has been shown to remain effective across the progression of sepsis in the data set presented, further validation is desired.

Existing work has been performed on estimating the ESPVR (Chen et al., 2001) and EDPVR (Klotz et al., 2006) using single-beat methods and echocardiography. However, these methods broadly require continuous echocardiography, relying on continuous stroke volume and ejection fraction information, which is cost prohibitive for implementation ICU wide (Ferrandis et al., 2013). In contrast, the method presented here utilises only a short echocardiography calibration, allowing sharing of equipment, and is independent of continuous stroke volume or ejection fraction measurements. Other supplementary measurements are also frequently required such as arm cuff pressures (Chen et al., 2001). Finally, these methods focus on presenting a single relationship rather than the unified set of cardiac dynamic information provided by a PV loop.

4.2 Stroke Work

The stroke work percentage errors in Table 3 compare two methods of approximating stroke work to directly measured stroke work. Estimated stroke work, from the estimated PV loop, exhibited notable errors, with medians of 15.6-41.2%. These errors, while non-negligible, still represent an improvement over the errors associated with a simplified stroke work metric in Eq. 11 in 11 of 15 quartiles evaluated. Overall, the average 25th percentile, median and 75th percentile errors were also reduced.

The correlation plots in Fig. 4 show estimated stroke work effectively captured trends in the measured stroke work. The average R value was 0.83, representing a strong correlation. These strong correlation coefficients, which are sustained over a variety of significant changes in subject condition, suggest the method can effectively be used to track changes in stroke work. This outcome is of major importance when monitoring patients.

There is some discrepancy between the low error values in Tables 1 – 2 and high correlation coefficients in Fig. 4, which imply the method is

effectively simulating PV loops, and the relatively high error values in Table 3, suggesting the opposite. The most likely explanation is that while points are located correctly, the generic waveforms do not always effectively match the contours of the measured waveforms. This outcome is somewhat expected due to the simplicity of the method and its minimal data input requirements

The example PV loops provided in Fig. 5 show that the method is able to capture the general shape and position of the driver function relatively effectively. The examples in Fig. 5 cover 25th percentile, median and 75th percentile absolute percentage error in stroke work estimation. As such, they show that, even at relatively high percentage errors, the method is still able to provide a relatively effective approximation of the shape and position of the PV loop. This, combined with the high R values in Fig. 4 suggest the method can consistently provide an indicator of relative if not necessarily absolute patient condition.

The positive bias in some cases (Fig 2) and negative bias in others (Figs 3 and 4) suggests the approximation does an overall reasonable job of estimating central behaviour, but is unable to capture the variety of subject-specific cardiac waveforms that can occur. That this bias seems clustered suggests it is due to each individual having a waveform shape that does not necessarily change significantly over their time monitored, but also does not conform to a sine wave. It may be possible to capture this baseline ventricular waveform during the echocardiography calibration, and use it instead of sine waves to simulate V_{lv} continuously. This approach would capture of this ‘characteristic’ subject-specific behaviour and add more detail to the method inputs to overcome this issue.

There exist single-beat methods to estimate Preload Recrutable Stroke Work (PRSW), which has been shown to have a strong correlation with measured stroke work, using non-invasive measurements and echocardiography (Karunanithi and Feneley, 2000). This approach was shown to perform well using invasive measurements in dogs (Karunanithi and Feneley, 2000). Invasive validation on humans showed similarly strong performance, but use of non-invasive measurements resulted in a fall in correlations between the estimated and measured PRSW to $R = 0.66$ (associated percentage errors aren’t reported) (Lee et al., 2003), lower than the method presented here ($R = 0.83$). Further, this method requires more expensive, continuous echocardiography (Ferrandis et al., 2013), as opposed a short echocardiography calibration. Finally, this

method does not provide the unified set of absolute pressure, volume and P-V contour information provided by the method presented here.

Overall the errors in Tables 1 – 2 suggest the method can be used to correctly locate a PV loop. The high correlation coefficients in Fig. 4 suggest the method can be used to effectively track changes in patient stroke work, and thus patient condition. Further, the method provides a reduction in errors associated with approximating stroke work in 11 of 15 assessed quartiles compared to a current method. It also provides an additional detailed plot, as opposed to a single lumped metric value. These overall outcomes provide a body of support for the validity and utility of the method.

4.3 Limitations

There are several limitations to this study that should be considered. First, it relies on a short initial calibration period of approximately 100 beats, during which echocardiography or similar is required. While echocardiography equipment is becoming more available in the modern ICU (Vieillard-Baron et al., 2008), and this process is non-invasive, this requirement still prevents full implementation of the method without a modest additional clinical workload using normal ICU instrumentation.

In addition, the data presented in this study is the product of a single protocol, which involved a single, but complex and varied (Nguyen et al., 2006), condition (sepsis), and several standardised interventions. This data set encompasses a range of subjects and behaviour, covering the full progression a healthy cardiac system to cardiac failure, including clinically standard ventilation and fluid interventions. However, there are a much larger range of possible cardiac conditions. The method would thus benefit from testing using different protocols involving different cardiac conditions. However, the overall physiology and assumptions used to develop this method would be largely expected to generalise to other cardiac conditions, as no condition or intervention specific assumptions are made.

Finally, the method requires validation in human subjects. However, a number of similar studies on single-beat approximations of cardiac dynamics have compared human and animal dynamics and found strong similarities between them (Karunanithi and Feneley, 2000, Lee et al., 2003, Klotz et al., 2006). This suggests the method, which is built on similar principles and encompasses the same physical system, should transfer effectively to human physiology.

5 CONCLUSIONS

A minimally invasive method for estimating PV loops beat-to-beat was developed. This method was validated over a cohort of 5 pure Piétrain pigs, which were subject to a protocol designed to exhibit a diverse range of cardiac states and levels of health. The method demonstrated the ability to effectively locate the four ‘edges’ of the PV loop, with low overall median errors for End-Systolic Volume (4.4%), End-Diastolic Volume (7.0%), Mean-Systolic Pressure (16.9%) and Mean-Diastolic Pressure (4.9%). While the method was able to accurately capture trends in stroke work (average R value of 0.83), there were notable errors when directly estimating stroke work values (median of 23.6%). While the method requires validation in human subjects, it has promise as a means of providing additional real time insight into cardiac behaviour at a patient bedside, without requiring additionally invasive instrumentation.

REFERENCES

- Angus, D. C., Linde-Zwirble, W. T., Lidicker, J., Clermont, G., Carcillo, J. & Pinsky, M. R. 2001. Epidemiology of Severe Sepsis in the United States: Analysis of Incidence, Outcome, and Associated Costs Of Care. *Critical Care Medicine*, 29, 1303-1310.
- Baan, J. & Van Der Velde, E. T. 1988. Sensitivity of Left Ventricular End-Systolic Pressure-Volume Relation to Type of Loading Intervention in Dogs. *Circulation Research*, 62, 1247-1258.
- Broscheit, J.-A., Weidemann, F., Strotmann, J., Steendijk, P., Karle, H., Roewer, N. & Greim, C.-A. 2006. Time-Varying Elastance Concept Applied To The Relation Of Carotid Arterial Flow Velocity And Ventricular Area. *Journal of Cardiothoracic and Vascular Anesthesia*, 20, 340-346.
- Burkhoff, D., De Tombe, P. P. & Hunter, W. C. 1993. Impact of Ejection on Magnitude and Time Course of Ventricular Pressure-Generating Capacity. *American Journal of Physiology-Heart and Circulatory Physiology*, 265, H899-H909.
- Burkhoff, D. & Sagawa, K. 1986. Ventricular Efficiency Predicted By an Analytical Model. *American Journal of Physiology-Regulatory, Integrative and Comparative Physiology*, 250, R1021-R1027.
- Chatterjee, K. 2009. The Swan-Ganz Catheters: Past, Present, and Future A Viewpoint. *Circulation*, 119, 147-152.
- Chen, C.-H., Fetcs, B., Nevo, E., Rochitte, C. E., Chiou, K.-R., Ding, P.-A., Kawaguchi, M. & Kass, D. A. 2001. Noninvasive Single-Beat Determination of Left Ventricular End-Systolic Elastance in Humans. *Journal of the American College of Cardiology*, 38, 2028-2034.

- Davidson, S., Pretty, C., Pironet, A., Desai, T., Janssen, N., Lambermont, B., Morimont, P. & Chase, J. G. 2016. Estimation of Ventricular Dead Space Volume through Use of Frank-Starling Curves. *Journal of Physiology (London) (In Review)*.
- Ferrandis, M.-J., Ryden, I., Lindahl, T. L. & Larsson, A. 2013. Ruling out Cardiac Failure: Cost-Benefit Analysis of a Sequential Testing Strategy with Nt-Probnp before Echocardiography. *Upsala Journal of Medical Sciences*, 118, 75-79.
- Frazier, S. K. & Skinner, G. J. 2008. Pulmonary Artery Catheters: State of the Controversy. *Journal of Cardiovascular Nursing*, 23, 113-121.
- Hall, J. E. 2010. *Guyton and Hall Textbook of Medical Physiology*, Elsevier Health Sciences.
- Jardin, F., Farcot, J.-C., Boisante, L., Curien, N., Margairaz, A. & Bourdarias, J.-P. 1981. Influence of Positive End-Expiratory Pressure on Left Ventricular Performance. *New England Journal of Medicine*, 304, 387-392.
- Kamoi, S., Pretty, C., Docherty, P., Squire, D., Revie, J., Chiew, Y. S., Desai, T., Shaw, G. M. & Chase, J. G. 2014. Continuous Stroke Volume Estimation from Aortic Pressure Using Zero Dimensional Cardiovascular Model: Proof of Concept Study from Porcine Experiments.
- Karunanithi, M. K. & Feneley, M. P. 2000. Single-Beat Determination of Preload Recrutable Stroke Work Relationship: Derivation and Evaluation in Conscious Dogs. *Journal of the American College of Cardiology*, 35, 502-513.
- Kastrup, M., Markewitz, A., Spies, C., Carl, M., Erb, J., Grosse, J. & Schirmer, U. 2007. Current Practice of Hemodynamic Monitoring and Vasopressor and Inotropic Therapy in Post-Operative Cardiac Surgery Patients in Germany: Results from a Postal Survey. *Acta Anaesthesiologica Scandinavica*, 51, 347-358.
- Klabunde, R. 2011. *Cardiovascular Physiology Concepts*, Lippincott Williams & Wilkins.
- Klotz, S., Hay, I., Dickstein, M. L., Yi, G.-H., Wang, J., Maurer, M. S., Kass, D. A. & Burkhoff, D. 2006. Single-Beat Estimation of End-Diastolic Pressure-Volume Relationship: A Novel Method with Potential for Noninvasive Application. *American Journal of Physiology-Heart and Circulatory Physiology*, 291, H403-H412.
- Lang, R. M., Badano, L. P., Mor-Avi, V., Afilalo, J., Armstrong, A., Ernande, L., Flachskampf, F. A., Foster, E., Goldstein, S. A. & Kuznetsova, T. 2015. Recommendations For Cardiac Chamber Quantification By Echocardiography In Adults: An Update From The American Society Of Echocardiography And The European Association Of Cardiovascular Imaging. *Journal of the American Society of Echocardiography*, 28, 1-39. E14.
- Lee, W.-S., Huang, W.-P., Yu, W.-C., Chiou, K.-R., Ding, P. Y.-A. & Chen, C.-H. 2003. Estimation of Preload Recrutable Stroke Work Relationship by a Single-Beat Technique in Humans. *American Journal of Physiology-Heart and Circulatory Physiology*, 284, H744-H750.
- Little, W., Cheng, C., Mumma, M., Igarashi, Y., Vinten-Johansen, J. & Johnston, W. 1989. Comparison Of Measures Of Left Ventricular Contractile Performance Derived From Pressure-Volume Loops In Conscious Dogs. *Circulation*, 80, 1378-1387.
- Little, W. C. 1985. The Left Ventricular Dp/Dtmax-End-Diastolic Volume Relation in Closed-Chest Dogs. *Circulation Research*, 56, 808-815.
- Mozaffarian, D., Benjamin, E. J., Go, A. S., Arnett, D. K., Blaha, M. J., Cushman, M., Das, S. R., De Ferranti, S., Després, J.-P. & Fullerton, H. J. 2015. Heart Disease and Stroke Statistics—2016 Update A Report from The American Heart Association. *Circulation*, Cir. 0000000000000350.
- Nguyen, H. B., Rivers, E. P., Abrahamian, F. M., Moran, G. J., Abraham, E., Trzeciak, S., Huang, D. T., Osborn, T., Stevens, D. & Talan, D. A. 2006. Severe Sepsis and Septic Shock: Review of the Literature and Emergency Department Management Guidelines. *Annals of Emergency Medicine*, 48, 54. E1.
- Pineda, L. A., Hathwar, V. S. & Grant, B. J. 2001. Clinical Suspicion of Fatal Pulmonary Embolism. *Chest Journal*, 120, 791-795.
- Sagawa, K. 1981. Editorial: The End-Systolic Pressure-Volume Relation Of The Ventricle: Definition, Modifications And Clinical Use. *Circulation*, 63.
- Senzaki, H., Chen, C.-H. & Kass, D. A. 1996. Single-Beat Estimation of End-Systolic Pressure-Volume Relation in Humans A New Method with the Potential for Noninvasive Application. *Circulation*, 94, 2497-2506.
- Stevenson, D., Revie, J., Chase, J. G., Hann, C. E., Shaw, G. M., Lambermont, B., Ghuysen, A., Kolh, P. & Desai, T. 2012a. Algorithmic Processing Of Pressure Waveforms to Facilitate Estimation of Cardiac Elastance. *Biomedical Engineering Online*, 11, 1-16.
- Stevenson, D., Revie, J., Chase, J. G., Hann, C. E., Shaw, G. M., Lambermont, B., Ghuysen, A., Kolh, P. & Desai, T. 2012b. Beat-To-Beat Estimation of the Continuous Left and Right Cardiac Elastance from Metrics Commonly Available in Clinical Settings. *Biomedical Engineering Online*, 11, 73.
- Suga, H. 1990. Ventricular Energetics. *Physiological Reviews*, 70, 247-277.
- Suga, H., Sagawa, K. & Shoukas, A. A. 1973. Load Independence of the Instantaneous Pressure-Volume Ratio of the Canine Left Ventricle and Effects of Epinephrine and Heart Rate on the Ratio. *Circulation Research*, 32, 314-322.
- Vieillard-Baron, A., Slama, M., Cholley, B., Janvier, G. & Vignon, P. 2008. Echocardiography in the Intensive Care Unit: From Evolution to Revolution? *Intensive Care Medicine*, 34, 243-249.
- Vincent, J.-L. & Gerlach, H. 2004. Fluid Resuscitation in Severe Sepsis and Septic Shock: An Evidence-based Review. *Critical Care Medicine*, 32, S451-S454.